Membership of The Physiological Society

The Physiological Society has over 2000 Members worldwide. Ordinary membership supports the careers of individuals who hold an appointment in physiology at postdoctoral level and are active in research. Benefits include:

- Free online access to *The Journal of Physiology* and *Experimental Physiology*
- Free or discounted attendance at Society Meetings
- Eligibility for grants from The Society
- Quarterly magazine *Physiology News* (online or hard copy)
- Wide variety of scientific events
- Free notices and programmes for all Society Meetings
- Ability to introduce guests to Society Meetings
- Access to a wide range of Special Interest Groups
- Full voting rights at General Meetings

The Society also supports individuals with different interests and levels of expertise in the discipline:

- ***Affiliate*** (graduate student or newly qualified postdoctoral workers)
- ***Associate*** (individuals with a background in physiology who do not qualify for Ordinary, Affiliate or Undergraduate membership)
- ***School and College Associate*** (secondary and college educators)
- ***Undergraduate Associate*** (individuals or groups of undergraduates keen to set up their own society)

For full details of all membership categories and details on how to join go to: www.physoc.org/membership

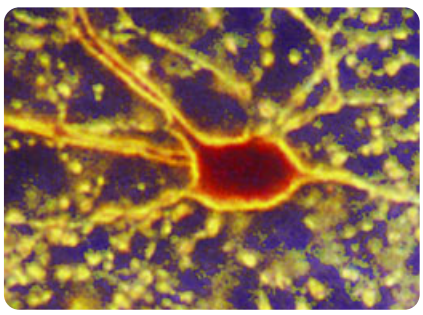

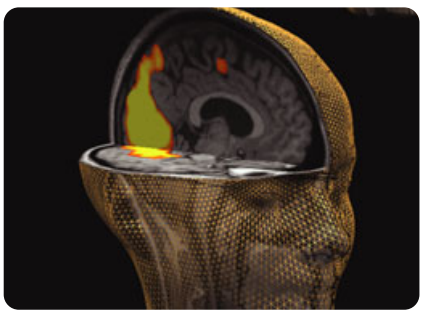

The Physiological Society

Advancing the science of life

aptara | TJP | tjp˙4180 | Dispatch: October 4, 2010 | CE: N / A
Journal | MSP No. | No. of pages: 14 | PE: Richard

Q1

Differential effects of Na^+–K^+ ATPase blockade on cortical layer V neurons

Trent R. Anderson, John R. Huguenard and David A. Prince

Neurology and Neurological Sciences and Molecular and Cellular Physiology, Stanford University, CA, USA

Sodium–potassium ATPase ('Na^+–K^+ ATPase' below) contributes to the maintenance of the resting membrane potential and the transmembrane gradients for Na^+ and K^+ in neurons. Activation of Na^+–K^+ ATPase may be important in controlling increases in intracellular sodium during periods of increased neuronal activity. Down-regulation of Na^+–K^+ ATPase activity is implicated in numerous CNS disorders, including epilepsy. Although Na^+–K^+ ATPase is present in all neurons, little is known about its activity in different subclasses of neocortical cells. We assessed the physiological properties of Na^+–K^+ ATPase in fast-spiking (FS) interneurons and pyramidal (PYR) cells to test the hypothesis that Na^+–K^+ ATPase activity would be relatively greater in neurons that generated high frequency action potentials (the FS cells). Whole-cell patch clamp recordings were made from FS and PYR neurons in layer V of rat sensorimotor cortical slices maintained *in vitro* using standard techniques. Bath perfusion of Na^+–K^+ ATPase antagonists (ouabain or dihydro-ouabain) induced either a membrane depolarization in current clamp, or inward current under voltage clamp in both cell types. PYR neurons were divided into two subpopulations based on the amplitude of the voltage or current shift in response to Na^+–K^+ ATPase blockade. The two PYR cell groups did not differ significantly in electrophysiological properties including resting membrane potential, firing pattern, input resistance and capacitance. Membrane voltage responses of FS cells to Na^+–K^+ ATPase blockade were intermediate between the two PYR cell groups ($P < 0.05$). The resting Na^+–K^+ ATPase current density in FS interneurons, assessed by application of blockers, was 3- to 7-fold larger than in either group of PYR neurons. Na^+–K^+ ATPase activity was increased either through direct Na^+ loading via the patch pipette or by focal application of glutamate (20 mM puffs). Under these conditions FS interneurons exhibited the largest increase in Na^+–K^+ ATPase activity. We conclude that resting Na^+–K^+ ATPase activity and sensitivity to changes in internal Na^+ concentration vary between and within classes of cortical neurons. These differences may have important consequences in pathophysiological disorders associated with down-regulation of Na^+–K^+ ATPase and hyperexcitability within cortical networks.

(Received 30 April 2010; accepted after revision 6 September 2010; first published online 6 September 2010)
Corresponding author D. A. Prince: Stanford University School of Medicine, Stanford Medical Center, Room M016, 300 Pasteur Dr., Stanford, CA 94305-5122, USA. Email: daprince@stanford.edu

Abbreviations aCSF, artificial cerebrospinal fluid; DGR, direct glutamate response; DHO, dihydro-ouabain; FS, fast spiking; IB, intrinsically bursting; I_h, membrane potential sag, reflective of hyperpolarization-activated cation current; Na^+–K^+ ATPase, sodium–potassium ATPase; PYR, pyramidal; RS, regular spiking.

Introduction

Na^+–K^+ ATPase catalyses the transport of Na^+ and K^+ across the cell membrane and is important in establishing and maintaining the electrochemical gradient. The maintenance of this transmembrane gradient is vital to cell function at multiple levels, including Na^+-coupled reuptake of glutamate (Balcar, 2002; O'Shea, 2002), glucose utilization (Honegger & Pardo, 1999; Magistretti, 2006), signal transduction (Liang *et al.* 2006) and modulation of cellular excitability and synaptic transmission (Ross & Soltesz, 2001; Reich *et al.* 2004; Kim *et al.* 2007). Changes in Na^+–K^+ ATPase activity have been implicated in numerous CNS disorders (Lees, 1991; Kumar & Kurup, 2002), including those manifest by hyperexcitability such as epilepsy in humans (Rapport *et al.* 1975) and in several animal models of epileptogenesis (Donaldson *et al.* 1971; Anderson *et al.* 1994; Fernandes

 DOI: 10.1113/jphysiol.2010.191858

et al. 1996; Reime Kinjo *et al.* 2007). While the Na^+–K^+ ATPase is ubiquitously expressed in all neurons our understanding of its activity in different types of neocortical cells remains limited.

Pyramidal (PYR) neurons represent the major source of excitatory output from neocortical layer V, a lamina that is the site of origin of interictal epileptiform discharge in both acute and chronic models of neocortical epileptogenesis (Connors, 1984; Prince & Tseng, 1993; Hoffman *et al.* 1994). The spike output of PYR cells is closely regulated by the action of inhibitory fast-spiking (FS) interneurons that synapse predominantly on PYR somata and proximal dendrites (Tamas *et al.* 1997). Regulation of FS interneuronal excitability is therefore important to normal and pathophysiological neocortical activity. In comparison to PYR cells, FS interneurons have a much higher firing frequency and can generate a sustained output in excess of 500 Hz with little spike frequency adaptation (McCormick *et al.* 1985; Connors & Gutnick, 1990 for review). This suggests that they possess an efficient mechanism for clearing increased $[Na^+]$ that would accumulate, particularly in their axons that have a high surface to volume ratio, and potentially suppress action potential firing. Activation of Na^+–K^+ ATPase by increases in $[Na^+]_i$ would serve to maintain the capacity to fire at high rates. There is little information available with respect to differences in Na^+–K^+ ATPase activity in subgroups of neocortical neurons, even though such differences are important to the regulation of resting membrane potential, synaptic transmission, neuronal responses to injury and the development of hyperexcitability (Ross & Soltesz, 2000; Vaillend *et al.* 2002; Anderson *et al.* 2005). In the present experiments, we tested the hypothesis that FS interneurons have greater Na^+–K^+ ATPase activity than PYR neurons in layer V, both at rest and during periods of high cellular activity.

Methods

Slice preparation

Protocols for all experiments were approved by the Stanford Institutional Animal Care and Use Committee. The authors have read, and the experiments comply with, the policies and regulations of *The Journal of Physiology* (Drummond, 2009). Male Sprague–Dawley rats (postnatal days (P)13–P24) or CD-1(ICR) mice (P15–P25) were deeply anaesthetized with 50 mg kg^{-1} sodium pentobarbital and decapitated. Brains were removed and coronal cortical slices (350 μm thick) of the somatosensory cortex were cut on a vibratome (VT 1000S; Leica, Nussloch, Germany) in a 4°C carboxygenated (95% O_2–5% CO_2) 'cutting' solution containing the following (in mM): 234 sucrose, 11 glucose, 24 $NaHCO_3$, 2.5 KCl, 1.25 NaH_2PO_4, 10 $MgSO_4$ and 0.5 $CaCl_2$. Slices were hemisected and incubated for 1 h at 32°C in carboxygenated artificial CSF (aCSF) containing (in mM): 126 NaCl, 26 $NaHCO_3$, 2.5 KCl, 1.25 NaH_2PO_4, 2 $MgSO_4$, 2 $CaCl_2$ and 10 glucose, pH 7.4. Slices were then incubated at room temperature before being transferred to the recording chamber.

Electrophysiological recording

Slices submerged in aCSF were initially visualized under brightfield for identification of neocortical layer V (Paxinos & Watson, 1998). Whole-cell recordings were obtained from cortical pyramidal (PYR) neurons or fast-spiking (FS) interneurons using an upright microscope (Axioskop, Carl-Zeiss, Thornwood, NY, USA) fitted with infrared differential interference contrast optics. Regular spiking (RS) and intrinsically bursting (IB) PYR neurons were distinguished based on their current-clamp firing behaviour (Connors *et al.* 1982; Tseng & Prince, 1993; Guatteo *et al.* 1994). FS interneurons were identified visually by the lack of a large emerging apical dendrite and electrophysiologically by their firing behaviour in current clamp (McCormick *et al.* 1985). To facilitate identification of FS interneurons some recordings were made in transgenic mice in which the enhanced green fluorescent protein (EGFP) was specifically expressed in parvalbumin-positive neurons (Chattopadhyaya *et al.* 2004). These parvalbumin-containing cells were routinely identified electrophysiologically as FS interneurons. No difference was observed in data collected from rats or transgenic mice. All recordings were obtained at 32°C using borosilicate glass (WPI, Sarasota, FL, USA) microelectrodes (tip resistance, 2–3 MΩ) filled with intracellular solution containing the following (in mM): 70 potassium gluconate, 70 KCl, 2 NaCl, 10 Hepes, 10 EGTA, 2 $MgCl_2$. The estimated E_{Cl} was approximately −16 mV, resulting in inward $GABA_A$ currents at a holding potential of −70 mV. Substitution of the internal solution for one containing a more physiological $[Cl^-]_i$ (124 potassium gluconate, 16 KCl, 2 NaCl, 10 Hepes, 4 EGTA, E_{Cl} –52 mV) had no significant effect on the Na^+–K^+ ATPase-sensitive current. Internal solution pH was adjusted to 7.3 using KOH as required. For intracellular labelling, biocytin 0.3–1% was included in the internal solution and sections processed as previously described (Salin *et al.* 1995). The electrode capacitance and bridge circuit were appropriately adjusted. The series resistance (R_s) of neurons chosen for analysis ranged between 6 and 30 MΩ (<20% of membrane input resistance) and was monitored for stability. Membrane potential was not corrected for a calculated 10 mV liquid junction potential. For measurement of the voltage sag induced by hyperpolarizing activated cationic current, the difference between the peak and steady-state membrane voltage recorded in response to a 1 s, −150 pA transmembrane current step was measured.

The post-train afterhyperpolarization potential was measured from the peak hyperpolarized value to the recovered baseline following a 1 s, 150 pA depolarizing transmembrane current step. For frequency–current (f–I) slopes linear regressions were performed on plots of the average firing frequency against current (I) normalized to the threshold current ($I_{threshold}$) that reliably produced a train of action potentials (100 pA for PYR neurons, 250 pA for FS interneurons. Similarly, we calculated an adaptation index as $100 \times (1 - F_{last}/F_2)$, where F_{last} corresponds to the firing rate of the last interspike interval and F_2 the second interspike interval (modified from Tateno & Robinson, 2004). PYR neurons exhibited a high variability in the first interspike interval (in both PYR1 and PYR2 response groups) and as such the 2nd interval was chosen for analysis. A Multiclamp 700A patch-clamp amplifier (Axon Instruments, Union City, CA, USA) was used in either current- or voltage-clamp mode. Recordings were sampled at 20 kHz, filtered at 10 kHz, captured on an A–D interface (Digidata 1320A, Axon Instruments) and stored on a computer. Simultaneous continuous recordings were performed on a MiniDigi 1A, sampling at 1 kHz. For voltage-clamp recordings, the membrane potential was clamped at −70 mV. Data were analysed using pCLAMP (Axon Instruments), Origin (Microcal Software, Northampton, MA, USA), and Prism (GraphPad) software. Data are presented as means ± S.E.M. Statistical significance was tested with a one-way ANOVA with Tukey's multiple comparison test or a Student's paired t test. Differences were determined to be significant if $P < 0.05$. The Na^+–K^+ ATPase current density for each cell was calculated as: $(\Delta V_m/R_{in})/C_m$ where ΔV_m is the membrane depolarization induced by Na^+–K^+ ATPase blockade, R_{in} the input resistance determined from the voltage response to an applied hyperpolarizing current step (1 s, 25–50 pA) and C_m the total capacitance calculated from the integrated area of the current response to a 40 ms, −5 mV voltage step. Membrane depolarization (Fig. 1*B*) or peak current (Fig. 2*B*) induced in FS or PYR neurons by a 30 s application of 100 μM dihydro-ouabain (DHO) were best fitted to single or double peak Gaussian distributions with the equation: $y = y_0 + (A/(w \times \sqrt{(\pi/2)})) \times \exp(-2((x - xc)/w)^2)$. Plots were performed in Origin 7.0 (OriginLabs, Northampton, MA, USA) and goodness of fit tested by the calculated coefficient of determination (R^2) equal to: total sum of squares – residual sum of squares/total sum of squares.

Q3

Q4

Experimental solutions

2-Amino-5-phosphonopentanoic acid (D-APV; 50 μM), 6,7-dinitroquinoxaline-2,3-dione (DNQX, 20 μM), 4-ethylphenylamino-1,2-dimethyl-6-methylaminopyrimidinium chloride (ZD7288, 20 μM) and tetrodotoxin (TTX; 1.0 μM) were purchased from Ascent Scientific (Weston-super-Mare, UK), prepared from stock solutions and bath applied in various experiments. Cadmium chloride (200 μM), dihydro-ouabain (20–100 μM), picrotoxin (50 μM) and ouabain (1–100 μM) were purchased from Sigma-Aldrich (St Louis, MO, USA). NaCl was substituted for NaH_2PO_4 in experiments where cadmium was used. All vehicle concentrations (NaOH, DMSO, ethanol) were <0.5% of final and had no effect on recordings. For isolation of the Na^+–K^+ ATPase activity, D-APV, DNQX, TTX and picrotoxin were routinely bath applied unless otherwise noted. Inclusion of TTX significantly reduced the occurrence of spreading depression and/or anoxic depolarization that may accompany blockade of the Na^+–K^+ ATPase (Muller & Somjen, 2000; Anderson & Andrew, 2002); however, these events were observed in some cells that were eliminated from further analysis.

Q5

Na^+-loading experiments

To increase $[Na^+]_i$, glutamate (20 mM) was locally delivered through a patch pipette (2–3 MΩ) by pressure ejection (31 kPa, 0.02–1.0 s pulse). For these experiments, DNQX was omitted from the bathing solution to allow AMPA activation, while D-APV was maintained to limit the potential inhibition of the Na^+–K^+ ATPase by Ca^{2+} entering through activated NMDA receptors (Fukuda & Prince, 1992*a*). However, potential inhibition of the Na^+–K^+ ATPase in FS interneurons through activation of Ca^{2+}-permeable AMPA receptors (Angulo *et al.* 1999) could not be eliminated following glutamate application. Reproducibility of the glutamate responses was confirmed by monitoring responses elicited by two pre-puffs (0.1 s) prior to the test puff (1.0 s), all applied 30 s apart. These pre-puffs elicited short (<5 s), small amplitude (<200 pA) responses that fully recovered well before the delivery of the test puff. This stimulus sequence was repeated every 3 min for 3–5 trials and the results averaged. While the response to the 1st pre-pulse showed some variability, possibly due to a 'cold barrel' effect, the responses to the 2nd pre-pulse and test pulse were consistent across trials for puff durations ≤1 s. Responses to puff durations >1.0 s were inconsistent across trials and omitted from the analysis. For calculation of Na^+–K^+ ATPase activity, the averaged direct glutamate response (DGR) obtained in the presence of DHO was digitally subtracted from the control glutamate response using pCLAMP software (Axon Instruments). The resulting trace is the current sensitive to blockade with DHO and is indicative of the glutamate-induced Na^+–K^+ ATPase activity. Integration of this current will therefore yield the underlying Na^+–K^+ ATPase charge. Addition of the Ca^{2+} chelator BAPTA

to the patch electrode solution, bath perfusion of the Ca^{2+} channel antagonist cadmium (200 μM) and the hyperpolarization-activated mixed cationic channel (I_h) blocker ZD7288 (20 μM) had no effect on the Na^+–K^+ ATPase response to the glutamate puff. Therefore, data from cells exposed to these agents were grouped and analysed with those from cells whose recordings were obtained with normal pipette and bath solutions. In separate experiments, $[Na^+]_i$ was increased by partially substituting sodium gluconate for potassium gluconate in the patch electrode solution.

Results

Whole-cell recordings were obtained from 96 PYR and 71 FS neurons from layer V of sensorimotor cortex. Cells were both visually and electrophysiologically identified as previously described (Kawaguchi & Kubota, 1993; Cauli *et al.* 1997; Xiang *et al.* 1998; Bacci *et al.* 2003). Identification of FS interneurons was aided in the transgenic mice by the fluorescence of EGFP expressed in parvalbumin-positive neurons.

Resting Na^+–K^+ ATPase activity varies between different types of neocortical neurons

Bath perfusion of dihydro-ouabain (DHO, 100 μM) for 30 s to either PYR or FS neurons under current clamp evoked a membrane depolarization in all cells tested. In FS interneurons, DHO induced a mean peak depolarization of 5.2 ± 0.8 mV (Fig. 1*A*). In contrast, DHO perfusion elicited more variable depolarizations in PYR neurons (Fig. 1*A*, middle and bottom). The response amplitude distributions from FS interneurons ($n = 8$) were well fitted with a single peak Gaussian ($R^2 = 0.89$), while those of PYR neurons ($n = 19$) had a bimodal distribution ($R^2 = 0.99$) (Fig. 1*B*) (see Methods for more details). PYR neurons thus fell into two significantly different groups based on the amplitude of their DHO-induced membrane

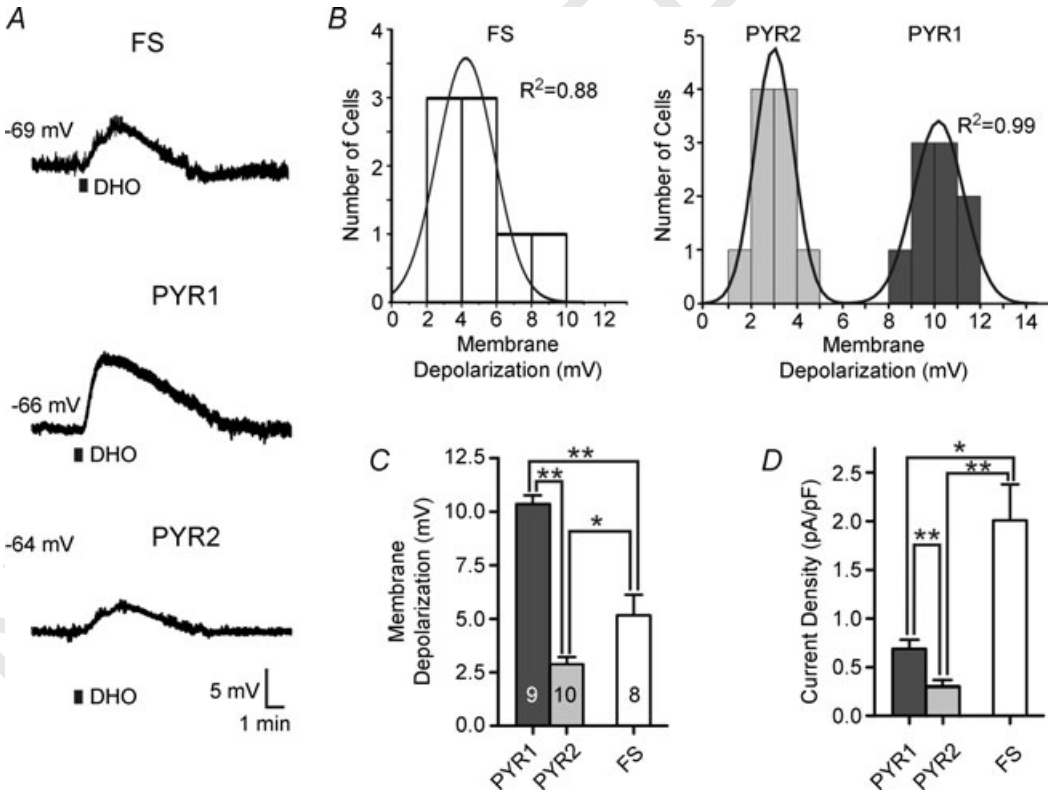

Figure 1. Dihydro-ouabain (DHO) induces a membrane depolarization in neocortical neurons
A, bath application of 100 μM DHO for 30 s induces a reversible membrane depolarization in a fast-spiking (FS) interneuron (top) and in two classes of pyramidal neuron (middle/bottom). Black bar represents period of DHO application. Resting membrane potential is listed to the left of each trace. *B*, population data of neuronal responses to DHO application. Left: data for FS interneurons are normally distributed (i.e. well fitted by a single peak Gaussian). Right: data for pyramidal neurons are best fitted by a 2-peak Gaussian. Goodness of fit calculated by the coefficient of determination (R^2). Note the clear separation of responses into large amplitude (termed PYR1) and small amplitude (termed PYR2) responses. *C*, mean (± S.E.M.) membrane depolarization in response to DHO for all cell types. *D*, calculated current density (current/capacitance) for all cell types. $^*P > 0.05$; $^{**}P > 0.01$.

Q6

depolarization. The mean peak amplitudes of responses in these two groups were 10.6 ± 0.4 mV (PYR1 neurons) and 2.7 ± 0.3 mV (PYR2 neurons) ($P < 0.0001$; Fig. 1*C*). We next examined the properties of these three cell groups (FS, PYR1 and PYR2) and their responses to Na^+–K^+ ATPase blockade in more detail.

Although responses to DHO application in PYR1 cells tended to have a faster rise time (1.7 ± 0.1 min) it was not significantly different from either the FS (1.9 ± 0.3 min) or the PYR2 (1.8 ± 0.2 min) groups ($P = 0.46$ and $P = 0.20$, respectively). As the recorded membrane depolarization may be sensitive to differences in cell size and permeability, we examined the current density for each cell type calculated from the input resistance, DHO-induced membrane depolarization and whole-cell capacitance (see Methods). This measure revealed that the Na^+–K^+ ATPase current density in FS interneurons (2.0 ± 0.4 pA pF^{-1}) was approximately 3–7 times greater than that in the PYR1 (0.7 ± 0.1 pA pF^{-1}) or PYR2 (0.3 ± 0.1 pA pF^{-1}) groups ($P < 0.01$ and $P < 0.001$, respectively; Fig. 1*D*). The PYR neuron groups were themselves significantly different from each other ($P < 0.01$). Similar results were also obtained when somatic surface areas were estimated from biocytin-filled cells of each group (data not shown). Thus, FS interneurons and PYR neurons differ in their sensitivity to Na^+–K^+ ATPase blockade, presumably due to differences in the resting state of their Na^+–K^+ ATPase activity.

The difference in resting Na^+–K^+ ATPase activity could be due to differences in the number of functional Na^+–K^+ ATPase molecules and/or a difference in rate of Na^+–K^+ ATPase activity. We included ATP/GTP in the internal pipette solution in an effort to increase and equalize the forward Na^+–K^+ ATPase rate across the different cell types (Gadsby & Nakao, 1989; Ross & Soltesz, 2000). The inclusion of ATP/GTP increased the amplitude of the response to DHO (100 μM) application above control levels in PYR neurons (15.2 ± 3.8 mV, $n = 10$) but had no effect on FS interneurons (5.3 ± 0.5 mV, $n = 5$). The lack of effect on FS interneurons suggests that the forward Na^+–K^+ ATPase rate is not limited by ATP/GTP levels in these neurons. Addition of ATP/GTP also hyperpolarized the resting membrane potential in PYR neurons (-67.5 ± 2.2 mV) and FS interneurons (-69.8 ± 1.3 mV). The inclusion of ATP/GTP in the patch pipette internal solution prevented grouping of the PYR neurons on the basis of their responses to blockade of the Na^+–K^+ ATPase with control internal solution as previously described (Fig. 1*B*). Consequently the data for PYR neurons were combined as no direct paired comparison with control data was possible. However, responses to blockade with DHO in PYR neurons loaded with ATP/GTP did fall into low (8.1 ± 0.7 mV, $n = 6$) and high (17.1 ± 2.9 mV, $n = 4$) amplitude groups. Independent of the PYR grouping, the results of this experiment clearly indicate that increasing intracellular ATP/GTP failed to equalize the DHO-sensitive Na^+–K^+ ATPase activity between PYR and FS neurons ($P < 0.05$). These results indicate that the difference in calculated Na^+–K^+ ATPase-dependent current density between cell types is primarily due to a difference in the number of Na^+–K^+ ATPase molecules in the cell membrane, rather than a difference in ATP/GTP limited rate.

To directly examine the current elicited by Na^+–K^+ ATPase blockade we conducted experiments under voltage clamp. At a holding potential of -70 mV, bath application of 100 μM DHO for 30 s induced a transient inward current in all cell groups. Increasing the duration of DHO application from 30 s to 5 min did not increase the amplitude of the response, but significantly reduced recovery to resting levels (data not shown). In FS interneurons, the responses were normally distributed with a mean ($\pm$ S.E.M.) peak inward current of 93.1 ± 12.1 pA ($n = 8$) (Fig. 2*A* and *B*). In PYR neurons, two groups could again be clearly identified. The first group of large amplitude responders (PYR1) had a mean peak inward current of 104.7 ± 5.5 pA ($n = 5$), while the second group (PYR2) had a smaller peak inward current of 26.1 ± 6.2 pA ($n = 5$) that was significantly different from the FS interneurons ($P < 0.001$) and the PYR1 group ($P < 0.0001$). Finally, responses to a series of drug concentrations were tested using DHO and a higher affinity Na^+–K^+ ATPase antagonist, ouabain (Fig. 2*C*). In FS interneurons, 20 μM DHO induced an inward current (52.9 ± 16.4 pA, $n = 4$) that was significantly smaller than that elicited by 100 μM DHO (93.1 ± 12.1 pA as above, $P < 0.05$). Inward currents elicited by application of 20 or 100 μM ouabain (124.2 ± 19.8 pA, $n = 6$ and 108.8 ± 7.4 pA, $n = 5$, respectively) were not significantly different from those induced by 100 μM DHO ($P = 0.44$). In PYR neurons, application of 20 or 50 μM DHO induced inward currents of 18.5 ± 1.3 pA ($n = 3$) and 27.4 ± 6.9 pA ($n = 4$), respectively. Interestingly, the distinct grouping of PYR neuron responses was not present at either lower doses of DHO (20 and 50 μM) or at a higher dose of ouabain (100 μM). The two groups of PYR cell responses were again evident when 20 μM ouabain (PYR1 $= 152.0 \pm 14.7$ pA, $n = 5$, PYR2 $= 45.0 \pm 3.8$ pA, $n = 6$) was applied ($P < 0.0001$). This suggests that the observed difference in Na^+–K^+ ATPase density between the two groups of PYR neurons is accompanied by a differential sensitivity to blockade of the Na^+–K^+ ATPase by DHO or ouabain.

The intrinsic membrane properties of FS interneurons were significantly different from both PYR groups; however, there were no significant differences between the two PYR neuron groups (Table 1). Specifically, there was no correlation between the amplitude of the DHO-induced membrane depolarization and numerous intrinsic properties (Table 1). Using previously described

Q7

criteria (Connors *et al.* 1982) we classified the firing behaviour of the PYR neurons and found that they were predominantly regular spiking ($n = 16$), although a few intrinsically bursting neurons were recorded in both PYR groups ($n = 3$) (Fig. 3*A*, and Table 1). There was no correlation between firing behaviour, frequency–current plots or adaptation index and the amplitude of responses to DHO application. While DHO application induced an expected leftward shift in the membrane voltage–current curve (Fig. 3*B*), there was no significant DHO-induced change in the input resistance of the three cell types (Fig. 3*C*). The laminar location and morphological identity of 18 PYR neurons was confirmed with intracellular biocytin labelling. There were no distinct differences in location or general cell morphology (Fig. 3*D*). Consequently, the amplitude of the PYR neuron response to blockade of resting Na^+–K^+ ATPase activity was consistently used in the remaining experiments to classify the neurons as belonging to the PYR1 or PYR2 group.

Na^+–K^+ ATPase activity induced by increased intracellular Na^+ varies among classes of neocortical neurons

It is clear that both FS interneurons and PYR1 neurons have more active resting Na^+–K^+ ATPase activity than PYR2 neurons. However, only a portion of the total Na^+–K^+ ATPase molecules are phosphorylated and thus active at rest and sensitive to pharmacological blockade (Forbush & Hoffman, 1979; Antonelli *et al.* 1989). To test the Na^+–K^+ ATPase capacity of the different cell groups we induced Na^+–K^+ ATPase activity by intracellularly loading cells with Na^+ using two methods. First, we focally applied 20 mM glutamate to slices while recording the resulting neuronal currents in FS and PYR neurons. In previous experiments in hippocampus, similar glutamate puffs were shown to be an indicator of Na^+–K^+ ATPase activity (Thompson & Prince, 1986; Fukuda & Prince, 1992*a*,*b*). In the present experiments under voltage clamp, the glutamate puff induced a fast, large inward current that quickly decayed, followed by a transient outward

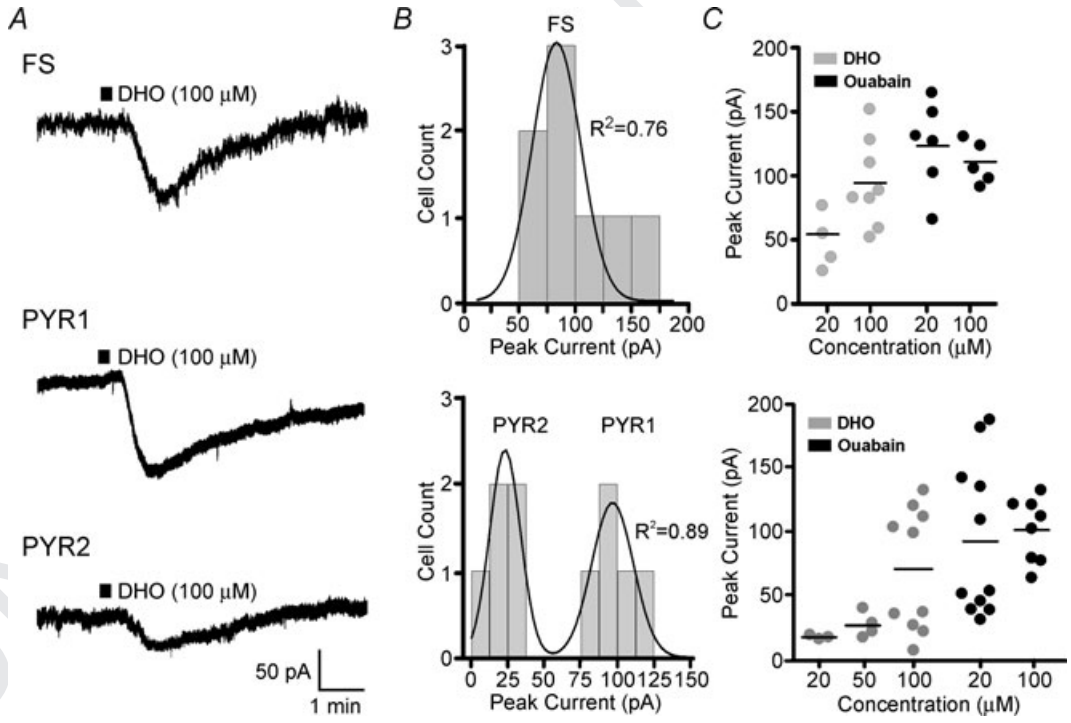

Figure 2. Heterogeneous inward current responses to Na^+–K^+ ATPase blockade in different classes of neocortical neurons
A, whole-cell voltage clamp responses to brief (30 s, black bar) application of 100 μM DHO, which induced a reversible inward current in all tested neurons. FS interneurons again showed an intermediate amplitude response between the two identified pyramidal types (larger amplitude (PYR1) and smaller amplitude (PYR2)). *B*, histograms of population responses to DHO in either the FS or PYR neurons. Again, the FS data were best fitted by a single peak Gaussian, and the PYR neurons by a 2-peak Gaussian. *C*, scatter plots of peak current responses to 30 s application of either the low affinity Na^+–K^+ ATPase antagonist DHO (grey symbols; 20, 50 or 100 μM) or the high affinity Na^+–K^+ ATPase antagonist ouabain (black symbols; 20, 100 μM) in FS (top) or PYR (bottom) neurons. Horizontal bars: mean values.

Table 1. Intrinsic membrane properties of different groups of recorded neurons

	PYR1 ($n = 9$)	PYR2 ($n = 10$)	FS ($n = 8$)
DHO – membrane depolarization (mV)	10.0 ± 0.4*	2.7 ± 0.3	5.2 ± 0.8†*
Resting membrane potential (mV)	−64.1 ± 0.9	−62.0 ± 1.3	−67.4 ± 1.5*
Input resistance (MΩ)			
Control	119.7 ± 19.5	116.6 ± 15.8	80.9 ± 8.5†*
DHO	127.6 ± 20.5	129.8 ± 16.4	79.3 ± 8.4†*
Capacitance (pF)	125.5 ± 22.3	116.9 ± 13.5	38.2 ± 5.3†*
I_h (mV)	4.30 ± 0.8	4.35 ± 0.8	1.17 ± 0.3†*
Post-train AHP (mV)	4.32 ± 0.8	3.72 ± 0.7	0.95 ± 0.1†*
Firing properties			
Type (RS/IB)	8/1	8/2	
Mean firing frequency (Hz)	14.8 ± 2.6	14.1 ± 3.0	73.4 ± 35.3†*
f–I slope	7.4 ± 0.2	7.0 ± 0.4	120.8 ± 14.3†*
Adaptation index	18.5 ± 3.1	20.3 ± 4.8	9.1 ± 5.9
Mean age (postnatal days)	19.8 ± 3.0	17.8 ± 1.0	21.0 ± 0.9
(range)	(17–27)	(16–27)	(18–27)

Values ± *x* are means ± S.E.M. I_h, membrane potential sag, reflective of hyperpolarization-activated cation current; AHP, afterhyperpolarization potential; RS, regular spiking; IB, intrinsically bursting; *f–I*, frequency–current. Firing properties were calculated for the first depolarizing step (in 50 pA increments) that reliably produced action potentials (100 pA for PYR, 250 pA for FS).The *f–I* slope and adaptation index were calculated as described in the Methods. †$P < 0.05$ statistically different from PYR1. *$P < 0.05$ statistically different from PYR2.

current in all cells. An example from an FS interneuron is displayed in Fig. 4*A*, Control. The glutamate puff was then repeated during blockade of the Na^+–K^+ ATPase by bath application of 100 μM DHO. The resulting current is thus independent of Na^+–K^+ ATPase activity and results primarily from the direct glutamate response (DGR) mediated by ionotropic glutamate receptors (Fig. 4*A*, DGR). These DGR currents were then averaged and digitally subtracted from the average control responses thereby revealing the isolated DHO-sensitive Na^+–K^+ ATPase current (Fig. 4*A*, Na^+–K^+ ATPase Activity) (see Methods for further details). A comparison between the neuronal types (Fig. 4*B*) revealed that the Na^+–K^+ ATPase charge in FS interneurons (13.7 ± 2.2 nC, $n = 12$) was much greater than that in either PYR1 (2.8 ± 0.3 nC, $n = 3$) or PYR2 neurons (1.5 ± 0.6 nC, $n = 5$; $P < 0.05$). PYR neuron grouping was determined as above by the amplitude of the response to blockade of resting Na^+–K^+ ATPase activity. Next we tested for a potential difference in sensitivity to the glutamate puffs between neuronal groups by varying the duration of the glutamate puff (0.02–1.0 s) applied to each type of neuron. At glutamate puff durations of 0.5 s and greater, FS interneurons showed more Na^+–K^+ ATPase charge than either PYR cell type ($P < 0.05$; Fig. 4*C*). In contrast, no statistically significant difference between the PYR groups could be determined in the Na^+–K^+ ATPase charge for any puff duration tested (Fig. 4*C*).

Neocortical neurons differ in a wide range of properties (e.g. morphological, synaptic, receptor complement) that may differentially influence their sensitivity to activation by a glutamate puff. As stated, during blockade of the Na^+–K^+ ATPase with DHO, the resulting charge induced by a glutmate puff (Fig. 4*A*, middle) would be indicative of the cell's direct response to glutamate (DGR), independent of Na^+–K^+ ATPase activity. As a result, by normalizing the Na^+–K^+ ATPase charge (a measure of Na^+–K^+ ATPase-induced activity) to the DGR charge (a measure of non-Na^+–K^+ ATPase-induced activity), we obtained an estimate of the induced Na^+–K^+ ATPase activity independent of any variance in application or responsiveness to the glutamate puff across cell types. The results indicated that both FS and PYR1 neurons exhibited significantly greater normalized charge than PYR2 neurons ($P < 0.05$; Fig. 4*D*). This suggests that FS and PYR1 neurons are more sensitive to activation of Na^+–K^+ ATPase induced by increases in $[Na^+]_i$. Finally, a comparison of this measure of induced Na^+–K^+ ATPase activity (Na^+–K^+ ATPase charge/DHO charge) in individual cells against their respective resting Na^+–K^+ ATPase activity (DHO current) revealed a separation of the two PYR groups based on both resting and induced Na^+–K^+ ATPase activity and a similarity in response between FS and PYR1 neurons (Fig. 4*E*). Therefore, resting Na^+–K^+ ATPase activity is a strong indicator of induced Na^+–K^+ ATPase activity for these cell types.

To directly test the potential for differential sensitivity to Na^+-induced Na^+–K^+ ATPase activity across cell types, we increased the concentration of Na^+ in the patch pipette solution to 40 or 70 mM. These concentrations

are known to activate both the α1 and α3 Na^+–K^+ ATPase isoforms (Blanco & Mercer, 1998). We then compared the induced current resulting from perfusion with various concentrations of Na^+–K^+ ATPase antagonists in the Na^+-loaded neurons with that obtained using the control (2 mM Na^+) intracellular solution. After achieving whole-cell configuration, the cells were dialysed for a minimum of 10 min with the higher Na^+ internal solutions, and a stable baseline holding current achieved for a minimum of 3 min before a series of successive ouabain concentrations (1, 20 and 100 μM) were applied to each cell. Representative traces of responses to ouabain from PYR1- and PYR2-type neurons are shown in Fig. 5*A*. For these experiments, ouabain was chosen for its high affinity, and lack of washout. Therefore, stable baseline levels could be recorded for each concentration while minimizing the potential for partial drug washout. Two distinct groups of amplitude responses induced by 20 μM ouabain were evident in Na^+-loaded PYR neurons, consistent with the previous results obtained from non-loaded PYR neurons (Fig. 2*C*). Consequently, PYR grouping in these experiments was based on the amplitude of the response to 20 μM ouabain. Application of 1 μM ouabain had little effect on any of the cell types (Fig. 5*B*). When exposed to 20 or 100 μM ouabain, PYR1 neurons loaded with 70 mM Na^+ generated more current than comparably Na^+-loaded PYR2 or FS neurons (Fig. 5*B*). Interestingly, the percentage increase in response to 100 μM ouabain was similar for both PYR1 (199.5% of control levels) and PYR2 neurons (172.4% of control) loaded with 70 mM Na^+. This suggests that high internal Na^+ concentrations (70 mM) equally activate the available Na^+–K^+ ATPase molecules in both PYR groups, thereby supporting our initial finding that PYR1 neurons have a greater total number of Na^+–K^+ ATPase molecules than PYR2. PYR1 neurons were also more sensitive to Na^+ loading than PYR2 neurons, as internal perfusion with both 40 and 70 mM Na^+ increased the Na^+–K^+ ATPase

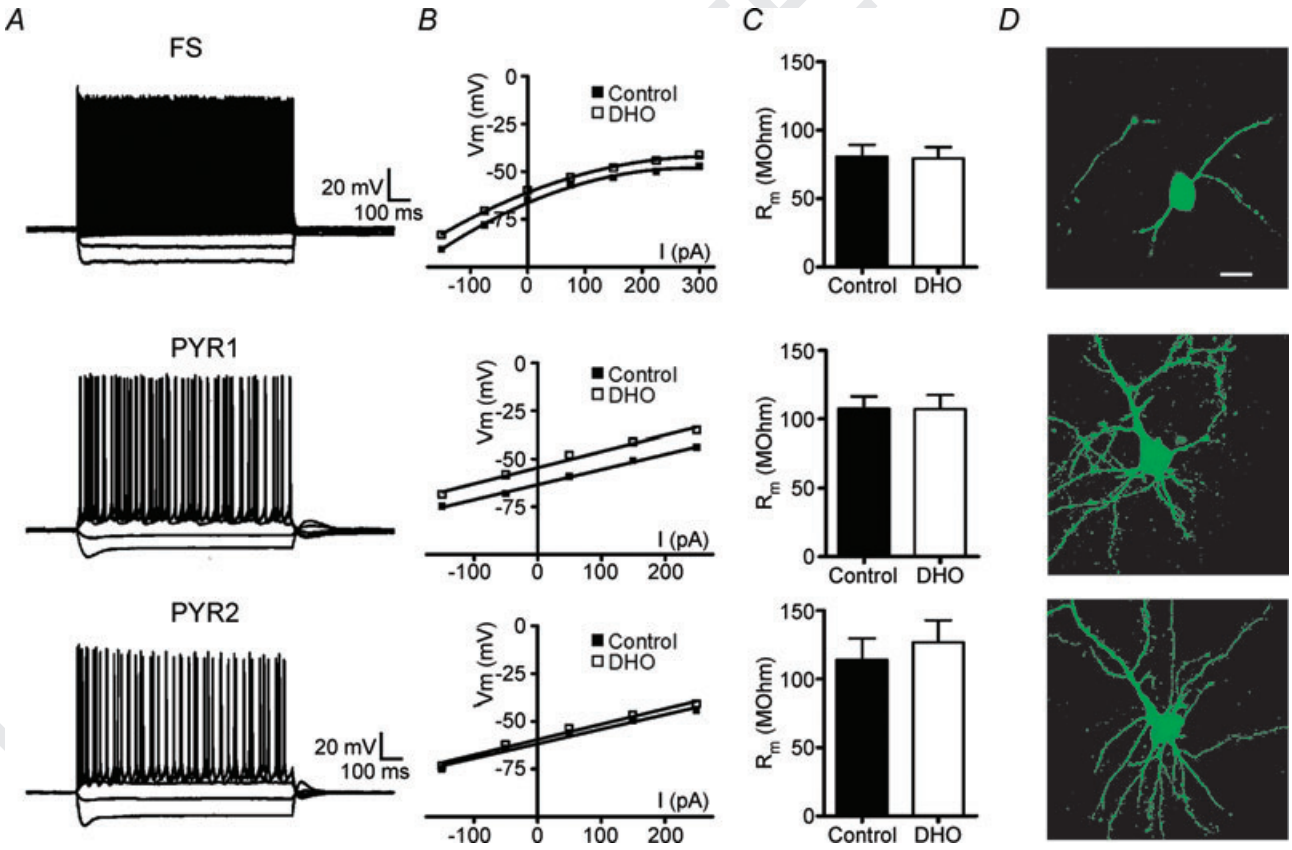

Figure 3. DHO does not alter input resistance in any of the different neuronal types
A, current clamp recordings in response to applied intracellular current steps (–150 to 300 pA, 1 s) in a FS, PYR1 or PYR2 neuron. Note the similarity in the recordings from both types of PYR neurons. *B*, *V–I* plots of cells recorded in *A* in control or during the peak membrane depolarization in response to DHO application (100 μM, 30 s). *C*, mean (± S.E.M.) membrane resistance (R_m) calculated from current steps applied in control or during DHO. Na^+–K^+ ATPase blockade by DHO did not significantly alter R_m in any of the cell types. Additionally, no difference was observed between the PYR1 and PYR2 groups ($P = 0.73$ control, $P = 0.33$ with DHO). *D*, representative biocytin-filled neurons of each recorded cell type. Scale bar: 20 μm applies for all images.

current blocked by 100 μM ouabain above the control value ($P < 0.05$; Fig. 5*B*). In FS interneurons, increases in internal Na^+ had no effect on the response to 1 or 20 μM ouabain. However, in FS cells loaded with 70 mM Na^+, the Na^+–K^+ ATPase current blocked by 100 μM ouabain was significantly increased (227.9 ± 17.6 pA) compared to that recorded in control 2 mM $[Na^+]_i$ (109.5 ± 9.5 pA) or 40 mM $[Na^+]_i$ (139.5 ± 4.6 pA) ($P < 0.01$; Fig. 5*B*).

Discussion

Na^+–K^+ ATPase activity in cortical neurons

We studied the activity of the Na^+–K^+ ATPase in cortical layer V fast-spiking (FS) interneurons and pyramidal (PYR) neurons to test the hypothesis that Na^+–K^+ ATPase function would vary between cell types and would be significantly more pronounced in fast-spiking interneurons. As expected, pharmacological blockade of the Na^+–K^+ ATPase resulted in a membrane depolarization under current clamp or an increase of inward current under voltage-clamp conditions. PYR cells could be clearly separated into two groups based on the amplitude of responses to blockade of Na^+–K^+ ATPase. PYR1 neurons comprised 48% of the PYR population and had significantly greater Na^+–K^+ ATPase-dependent currents than PYR2 cells. In contrast, the response of FS interneurons was homogeneous and intermediate in amplitude between that of the two groups of PYR neurons. However, when cell size (membrane capacitance) was taken into account, FS interneurons possessed a 3- to 7-fold greater Na^+–K^+ ATPase-dependent current density than either of the PYR groups. Despite their smaller cell size, the input resistance of FS interneurons is lower than that of PYR cells (Table 1) as previously reported (Angulo *et al.* 1999; Bacci *et al.* 2003). The higher density and level of resting Na^+–K^+

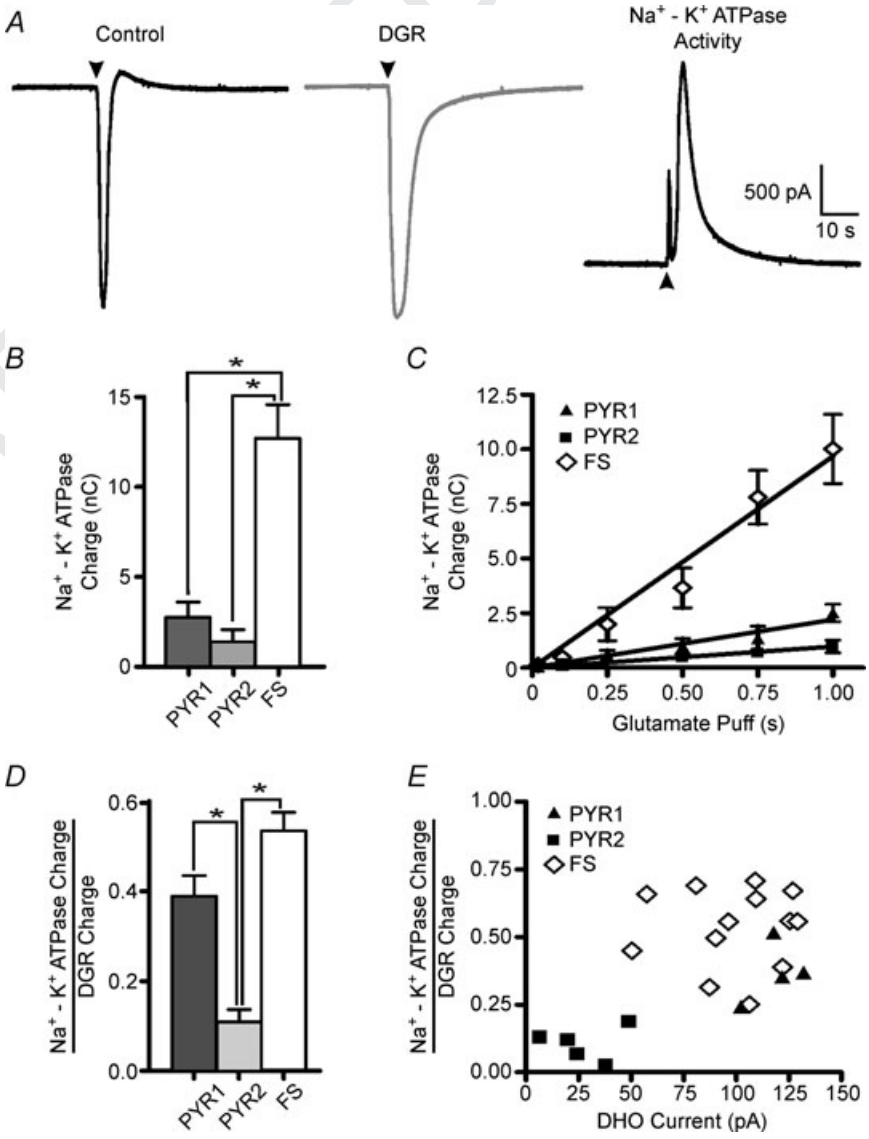

Figure 4. Glutamate puff-induced activation of the Na^+–K^+ ATPase
Glutamate (20 mM) was locally delivered through a patch-pipette by a brief pressure pulse (31 kPa, 1 s). *A*: left, representative trace from a FS interneuron under voltage clamp in response to a glutamate puff in control. Glutamate evoked a large amplitude, fast rising inward current followed by a rebound outward current. Middle, following blockade of the Na^+–K^+ ATPase with 100 μM DHO the glutamate puff is repeated and the DGR recorded. Right, digital subtraction of the DGR response from the control response reveals the underlying DHO-sensitive Na^+–K^+ ATPase current (Na^+–K^+ ATPase activity). *B*, mean (± S.E.M.) Na^+–K^+ ATPase charge for FS, PYR1 and PYR2 neurons calculated as the area under the Na^+–K^+ ATPase activity curve and then averaged across trials (see Methods for more details). PYR neurons were grouped based on the amplitude of the current induced by DHO as in Fig. 1. *C*, comparison of Na^+–K^+ ATPase charge for the three groups across multiple glutamate puff durations. *D*, an estimate of the fraction of Na^+–K^+ ATPase activity induced by the glutamate puff (Na^+–K^+ ATPase charge) against the total induced non-Na^+–K^+ ATPase activity (DGR charge) (mean ± S.E.M.). *E*, fractional glutamate puff-induced Na^+–K^+ ATPase activity is plotted against the resting Na^+–K^+ ATPase activity (DHO current). $^*P > 0.05$, $V_m = -70$ mV.

ATPase activity (Figs 1 and 3) could play a role in the maintenance of a more hyperpolarized resting membrane potential and maintenance of high frequency firing in FS cells in such 'leaky' neurons.

Under normal resting conditions only a portion of the total membrane-bound Na^+–K^+ ATPase is phosphorylated and available to contribute to the measured change in membrane voltage or current when the Na^+–K^+ ATPase is pharmacologically blocked. By increasing internal Na^+, either directly (pipette Na^+ loading) or indirectly (glutamate puff), we were able to assess each neuron's responsiveness to Na^+ and their capacity to activate the Na^+–K^+ ATPase. The result was greater activation of Na^+–K^+ ATPase-dependent currents in FS interneurons and PYR1 cells than in PYR2 neurons. In the glutamate puff experiments it was possible to compare the resting Na^+–K^+ ATPase activity, measured as the change in holding current during the initial Na^+–K^+ ATPase blockade, with the increased Na^+–K^+ ATPase-dependent current, measured as the component of charge induced by the glutamate puff that was sensitive to Na^+–K^+ ATPase block by DHO (Figs 4 and 5). In this way, the relationship between resting Na^+–K^+ ATPase activity and total Na^+–K^+ ATPase activity activated by a Na^+ load could be determined. FS and PYR1 neurons have both higher resting Na^+–K^+ ATPase activity and greater ability to increase Na^+–K^+ ATPase activity, allowing them to accommodate a wider range of Na^+ loads with increases in Na^+–K^+ ATPase activity.

The subgroups of PYR neurons differ in Na^+–K^+ ATPase activity but not intrinsic properties

It is clear from the experimental data that two distinct groups of PYR neurons with varying Na^+–K^+ ATPase activity exist in layer V cortex; however, we have been unable to detect any correlations between resting Na^+–K^+ ATPase activity and any measured electrophysiological property. Responses from both PYR groups were observed on the same day, from the same animal and with the same stock of Na^+–K^+ ATPase antagonists. As the Na^+–K^+ ATPase antagonists, especially ouabain, are difficult to wash out, we recorded from only one neuron per slice to be certain that residual Na^+–K^+ ATPase blockade was not contributing to our results. The presence of two distinct groups with no gradation in the distribution (Fig. 1*B*) helped rule out potential artifacts such as depth of recording in slice, slice health and/or drug penetration. Our data strongly suggest that the differences in recorded

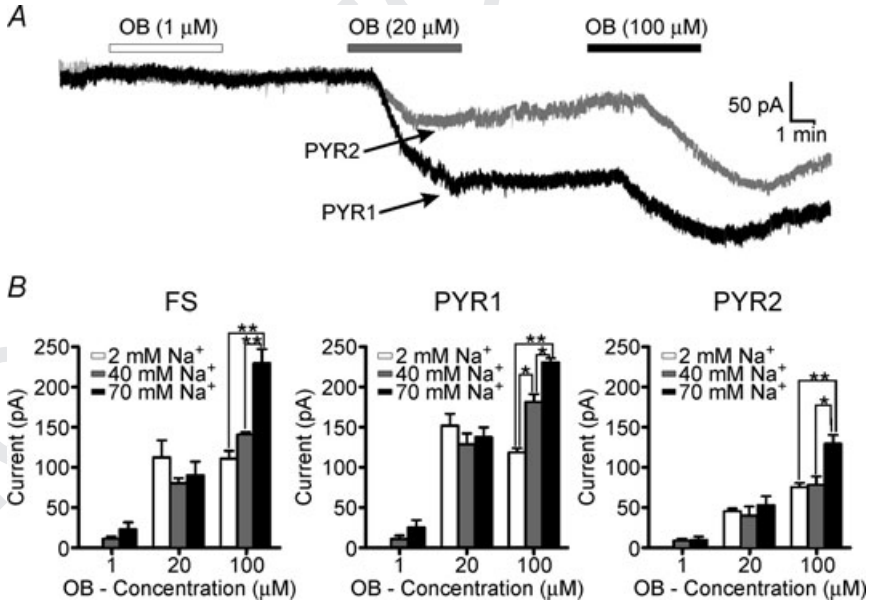

Figure 5. Increasing internal Na^+ concentration increases resting Na^+–K^+ ATPase activity in all cell types

A, voltage clamp trace from a PYR1 (black) or PYR2 (grey) neuron loaded with 70 mM Na^+ internally through the patch pipette. After sufficient time was allowed for dialysis of the Na^+ (> 10 min) and stability achieved in the baseline recording, ouabain (OB) was applied at various concentrations (1, 20 and 100 μM). Application of 20 μM ouabain produced two distinct groups of responses in PYR neurons, consistent with our previous findings in non-loaded neurons, and was used for PYR neuron grouping (PYR1 and PYR2). *B*, mean (± S.E.M.) current recorded from FS ($n = 18$), PYR1 ($n = 10$) or PYR2 ($n = 14$) neurons in different internal Na^+ concentrations. Cells were loaded with control (2 mM), 40 or 70 mM Na^+. Loading with 70 mM Na^+ increased the current induced by 100 μM, but not lower concentrations of ouabain, in all cell types. Only PYR1 neurons were more sensitive to 40 mM Na^+ compared to control (2 mM). $^*P > 0.05$, $^{**}P > 0.01$. $V_m = -70$mV.

Na^+–K^+ ATPase activity relate to differences in cell expression of Na^+–K^+ ATPase and not to artifacts of recording conditions, slice preparation or other intrinsic properties of the recorded PYR neurons. However, we cannot rule out more subtle differences in the electrophysiological properties or morphology of the PYR 1 and 2 subgroups not tested in this study.

The Na^+–K^+ ATPase is a protein multimer consisting of alpha (α) and beta (β) subunits (Lingrel, 1992). The α subunit has two neuronal forms (α1 and α3) that determine the major enzymatic and transporter properties of the molecule and confer sensitivity to blockade by Na^+–K^+ ATPase antagonists (i.e. ouabain and DHO). Specifically, the α3 subunit is less sensitive to changes in Na^+ and K^+ and is much more sensitive to activation by ATP and blockade by Na^+–K^+ ATPase antagonists than the α1 isoform (Blanco & Mercer, 1998). *In situ* analysis of the neocortex has shown protein levels for both the α1 and α3 isoform, with the α3 isoform being heavily expressed in PYR neurons (Hieber *et al.* 1991). In testing the sensitivity of PYR neurons to ouabain and DHO, we observed a distinct concentration range over which the PYR neuron grouping was evident. Low doses of ouabain (with high α3 affinity) separated the groups as did higher doses of DHO (with lower α3 affinity). Interestingly, higher doses of ouabain (100 μM) failed to separate the PYR groups. This concentration of ouabain (100 μM) would be expected to inhibit both the α1 and α3 isoforms (Blanco & Mercer, 1998). While the maximum Na^+–K^+ ATPase current induced by 100 μM ouabain was similar to that observed with 20 μM ouabain, the small amplitude current responses were no longer evident. In the Na^+-loading experiments, the PYR neurons with small responses to 20 μM ouabain (PYR2) also showed the smaller responses to 100 μM ouabain. These results suggest that the lack of grouping on resting Na^+–K^+ ATPase activity with low dose DHO (20 or 50 μM) may be due to PYR2 neurons being non-responsive to this level of Na^+–K^+ ATPase blockade. At higher doses a ceiling effect may be imposed such that the responses of PYR1 neurons are muted due to the limited number of Na^+–K^+ ATPase molecules active at rest and thus sensitive to blockade. The Na^+–K^+ ATPase capacity of PYR1 was not appreciated with modest challenges to the pump, but only observed when activated by a strong intracellular Na^+ load (70 mM) Taken together, these findings suggest that there is a difference in the isoform composition of the two PYR groups. This is also well supported by the observed differences in Na^+ and ATP sensitivity in the PYR neuron groups (Blanco & Mercer, 1998; Dobretsov & Stimers, 2005 for review). Similar results across neuronal subtypes have been recently reported in hippocampal subiculum neurons, where interneurons were more sensitive to blockade by ouabain than pyramidal neurons (Richards *et al.* 2007). The difference was attributed to differential expression of α isoforms of the Na^+–K^+ ATPase. Here we show that such a difference in α isoform expression may exist between and even *within* subtypes of neocortical neurons. This is in line with studies showing that the membrane density of Na^+–K^+ ATPase may vary between cell types and even within the membrane distribution of a single cell (Shyjan *et al.* 1990; Brines *et al.* 1991; Hieber *et al.* 1991; McGrail *et al.* 1991; Brines & Robbins, 1993). However, immunohistochemical results on biocytin-filled neurons from our experiments or from naive control animals were inconclusive. There was no apparent difference in association of the Na^+–K^+ ATPase α1 or α3 isoforms between FS and PYR neurons or within PYR neuron subtypes (data not shown). The inability to distinguish between FS and PYR neuron Na^+–K^+ ATPase immunoreactivity may be due to poor antibody penetration and/or the insensitivity of the antibody to detect small differences in membrane density that are more easily resolved at the electrophysiological level.

The Na^+–K^+ ATPase significantly contributes to the resting membrane potential. However, here we found no significant difference in resting membrane potential between the PYR1 and PYR2 groups – although there was a trend towards PYR1 being more hyperpolarized. Several factors may contribute to this finding. The PYR neurons may have similar net resting Na^+–K^+ ATPase activity but differ in relative α isoform-specific activity and thus sensitivity to blockade by the more α3-specific Na^+–K^+ ATPase antagonists. At present, to our knowledge, no α1-specific antagonists exist. Preliminary experiments with the new α3 isoform-specific antagonist, Agrin-95 (Hilgenberg *et al.* 2006) have yielded similar differences in FS and PYR neuron resting Na^+–K^+ ATPase activity to those described above. Actions of other ATPases (eg. K^+ or Ca^{2+}), transporters (eg. $Na^+/K^+/2Cl^-$ or Na^+/Ca^{2+}) or protein kinases may also differentially contribute in the PYR neuron groups. In addition, potential differences in local microenvironment (ionic or synaptic) due to architecture or even differences in glial localization may selectively alter the demand on resting Na^+–K^+ ATPase activity. The two populations of PYR cells may therefore express different densities and isoforms of the Na^+–K^+ ATPase to meet the challenges of their local environment.

The Na^+–K^+ ATPase is a dynamically regulated membrane protein whose expression is controlled by activity, endogenous inhibitors and several intracellular messengers (Ross & Soltesz, 2001; Therien & Blostein, 2000; Kang *et al.* 2003; Dobretsov & Stimers, 2005). Detailed testing of the intrinsic properties between the two groups of PYR neurons failed to reveal any significant differences that correlated with differences in their Na^+–K^+ ATPase activity. One possibility is that differences in local activity help to promote higher Na^+–K^+ ATPase levels in one group of PYR neurons than the other. For example, differences in Na^+–K^+ ATPase activity between neurons may reflect differences in the type or origin of

afferent synaptic input to subgroups of cells (Senatorov & Hu, 1997). Na^+–K^+ ATPase activity may both regulate and be regulated by release of several neurotransmitters (Phillis & Wu, 1981; Hernandez & Condes-Lara, 1992). The separation of the response of the PYR neurons into two electrophysiologically distinct groups required a relatively high dose of Na^+–K^+ ATPase antagonists. At these concentrations the Na^+–K^+ ATPase antagonists can cause neurotransmitter release and induce spreading depression if applied in the absence of NMDA antagonists or TTX (Muller & Somjen, 2000; Anderson & Andrew, 2002). In fact, glutamate has been shown to preferentially activate $\alpha 3$ on cerebellar and cerebral neurons (Dobretsov & Stimers, 2005). Therefore, in this study synaptic transmission was routinely blocked by bath application of D-APV, DNQX, picrotoxin and TTX. Although this aided in isolating the Na^+–K^+ ATPase activity without contamination by synaptic currents, it prevented a detailed study of the potential reciprocal regulation of synaptic transmission and Na^+–K^+ ATPase activity, or differences in synaptic input to the three groups of neurons examined here.

Conclusions

It is evident that expression of Na^+–K^+ ATPase varies across and within types of cortical neurons and that differences extend to the state of resting Na^+–K^+ ATPase activity as well as total Na^+–K^+ ATPase capacity. Differences in Na^+–K^+ ATPase activity within an otherwise homogeneous cell population would have an important impact on cellular function both at rest and especially during periods of high cellular activity. By defining the nature of these differences, we can begin to understand how they may contribute to control neuronal activities in functional states where there is increased demand for Na^+–K^+ ATPase activity. For example, FS and PYR1 neurons may be better equipped than PYR2 neurons to 'cope' with states of excessive activity, such as those that occur during epileptiform discharges. The potential adaptive or maladaptive effects of high or low Na^+–K^+ ATPase density and capacity during periods of hyperexcitability, and alterations in pathophysiological processes, such as those resulting from cortical injury and epileptogenesis, will be important to explore in future experiments.

References

Anderson TR & Andrew RD (2002). Spreading depression: imaging and blockade in the rat neocortical brain slice. *J Neurophysiol* **88**, 2713–2725.

Anderson TR, Jarvis CR, Biedermann AJ, Molnar C & Andrew RD (2005). Blocking the anoxic depolarization protects without functional compromise following simulated stroke in cortical brain slices. *J Neurophysiol* **93**, 963–979.

Anderson WR, Franck JE, Stahl WL & Maki AA (1994). Na,K-ATPase is decreased in hippocampus of kainate-lesioned rats. *Epilepsy Res* **17**, 221–231.

Angulo MC, Rossier J & Audinat E (1999). Postsynaptic glutamate receptors and integrative properties of fast-spiking interneurons in the rat neocortex. *J Neurophysiol* **82**, 1295–1302.

Antonelli MC, Baskin DG, Garland M & Stahl WL (1989). Localization and characterization of binding sites with high affinity for [^{3}H]ouabain in cerebral cortex of rabbit brain using quantitative autoradiography. *J Neurochem* **52**, 193–200.

Bacci A, Rudolph U, Huguenard JR & Prince DA (2003). Major differences in inhibitory synaptic transmission onto two neocortical interneuron subclasses. *J Neurosci* **23**, 9664–9674.

Balcar VJ (2002). Molecular pharmacology of the Na^+-dependent transport of acidic amino acids in the mammalian central nervous system. *Biol Pharm Bull* **25**, 291–301.

Blanco G & Mercer RW (1998). Isozymes of the Na-K-ATPase: heterogeneity in structure, diversity in function. *Am J Physiol Renal Physiol* **275**, F633–F650.

Brines ML, Gulanski BI, Gilmore-Hebert M, Greene AL, Benz EJ Jr & Robbins RJ (1991). Cytoarchitectural relationships between [^{3}H]ouabain binding and mRNA for isoforms of the sodium pump catalytic subunit in rat brain. *Brain Res Mol Brain Res* **10**, 139–150.

Brines ML & Robbins RJ (1993). Cell-type specific expression of Na^+,K^+-ATPase catalytic subunits in cultured neurons and glia: evidence for polarized distribution in neurons. *Brain Res* **631**, 1–11.

Cauli B, Audinat E, Lambolez B, Angulo MC, Ropert N, Tsuzuki K, Hestrin S & Rossier J (1997). Molecular and physiological diversity of cortical nonpyramidal cells. *J Neurosci* **17**, 3894–3906.

Chattopadhyaya B, Di Cristo G, Higashiyama H, Knott GW, Kuhlman SJ, Welker E & Huang ZJ (2004). Experience and activity-dependent maturation of perisomatic GABAergic innervation in primary visual cortex during a postnatal critical period. *J Neurosci* **24**, 9598–9611.

Connors BW (1984). Initiation of synchronized neuronal bursting in neocortex. *Nature* **310**, 685–687.

Connors BW & Gutnick MJ (1990). Intrinsic firing patterns of diverse neocortical neurons. *Trends Neurosci* **13**, 99–104.

Connors BW, Gutnick MJ & Prince DA (1982). Electrophysiological properties of neocortical neurons in vitro. *J Neurophysiol* **48**, 1302–1320.

Dobretsov M & Stimers JR (2005). Neuronal function and alpha3 isoform of the Na/K-ATPase. *Front Biosci* **10**, 2373–2396.

Donaldson J, St Pierre T, Minnich J & Barbeau A (1971). Seizures in rats associated with divalent cation inhibition of Na^+-K^+-ATP'ase. *Can J Biochem* **49**, 1217–1224.

Drummond GB (2009). Reporting ethical matters in *The Journal of Physiology*: standards and advice. *J Physiol* **587**, 713–719.

Fernandes MJ, Naffah-Mazzacoratti MG & Cavalheiro EA (1996). Na^+K^+ ATPase activity in the rat hippocampus: a study in the pilocarpine model of epilepsy. *Neurochem Int* **28**, 497–500.

Forbush B III & Hoffman JF (1979). Evidence that ouabain binds to the same large polypeptide chain of dimeric Na,K-ATPase that is phosphorylated from Pi. *Biochemistry* **18**, 2308–2315.

Fukuda A & Prince DA (1992*a*). Excessive intracellular Ca^{2+} inhibits glutamate-induced Na^+-K^+ pump activation in rat hippocampal neurons. *J Neurophysiol* **68**, 28–35.

Fukuda A & Prince DA (1992*b*). Postnatal development of electrogenic sodium pump activity in rat hippocampal pyramidal neurons. *Brain Res Dev Brain Res* **65**, 101–114.

Gadsby DC & Nakao M (1989). Steady-state current-voltage relationship of the Na/K pump in guinea pig ventricular myocytes. *J Gen Physiol* **94**, 511–537.

Guatteo E, Bacci A, Franceschetti S, Avanzini G & Wanke E (1994). Neurons dissociated from neocortex fire with 'burst' and 'regular' trains of spikes. *Neurosci Lett* **175**, 117–120.

Hernandez J & Condes-Lara M (1992). Brain Na^+/K^+-ATPase regulation by serotonin and norepinephrine in normal and kindled rats. *Brain Res* **593**, 239–244.

Hieber V, Siegel GJ, Fink DJ, Beaty MW & Mata M (1991). Differential distribution of (Na, K)-ATPase alpha isoforms in the central nervous system. *Cell Mol Neurobiol* **11**, 253–262.

Hilgenberg LG, Su H, Gu H, O'Dowd DK & Smith MA (2006). $\alpha 3Na^+/K^+$-ATPase is a neuronal receptor for agrin. *Cell* **125**, 359–369.

Hoffman SN, Salin PA & Prince DA (1994). Chronic neocortical epileptogenesis in vitro. *J Neurophysiol* **71**, 1762–1773.

Honegger P & Pardo B (1999). Separate neuronal and glial Na^+,K^+-ATPase isoforms regulate glucose utilization in response to membrane depolarization and elevated extracellular potassium. *J Cereb Blood Flow Metab* **19**, 1051–1059.

Kang TC, Hwang IK, Park SK, An SJ, Nam YS, Kim DH, Lee IS & Won MH (2003). Elevation of Na^+-K^+ ATPase immunoreactivity in GABAergic neurons in gerbil CA1 region following transient forebrain ischemia. *Brain Res* **977**, 284–289.

Kawaguchi Y & Kubota Y (1993). Correlation of physiological subgroupings of nonpyramidal cells with parvalbumin- and calbindinD28k-immunoreactive neurons in layer V of rat frontal cortex. *J Neurophysiol* **70**, 387–396.

Kim JH, Sizov I, Dobretsov M & von Gersdorff H (2007). Presynaptic Ca^{2+} buffers control the strength of a fast post-tetanic hyperpolarization mediated by the alpha3 Na^+/K^+-ATPase. *Nat Neurosci* **10**, 196–205.

Kumar AR & Kurup PA (2002). Inhibition of membrane Na^+-K^+ ATPase activity: a common pathway in central nervous system disorders. *J Assoc Physicians India* **50**, 400–406.

Lees GJ (1991). Inhibition of sodium-potassium-ATPase: a potentially ubiquitous mechanism contributing to central nervous system neuropathology. *Brain Res Brain Res Rev* **16**, 283–300.

Liang M, Cai T, Tian J, Qu W & Xie ZJ (2006). Functional characterization of Src-interacting Na/K-ATPase using RNA interference assay. *J Biol Chem* **281**, 19709–19719.

Lingrel JB (1992). Na,K-ATPase: isoform structure, function, and expression. *J Bioenerg Biomembr* **24**, 263–270.

McCormick DA, Connors BW, Lighthall JW & Prince DA (1985). Comparative electrophysiology of pyramidal and sparsely spiny stellate neurons of the neocortex. *J Neurophysiol* **54**, 782–806.

McGrail KM, Phillips JM & Sweadner KJ (1991). Immunofluorescent localization of three Na,K-ATPase isozymes in the rat central nervous system: both neurons and glia can express more than one Na,K-ATPase. *J Neurosci* **11**, 381–391.

Magistretti PJ (2006). Neuron-glia metabolic coupling and plasticity. *J Exp Biol* **209**, 2304–2311.

Muller M & Somjen GG (2000). Na^+ dependence and the role of glutamate receptors and Na^+ channels in ion fluxes during hypoxia of rat hippocampal slices. *J Neurophysiol* **84**, 1869–1880.

O'Shea RD (2002). Roles and regulation of glutamate transporters in the central nervous system. *Clin Exp Pharmacol Physiol* **29**, 1018–1023.

Paxinos G & Watson (1998). *The Rat Brain in Stereotactic Coordinates*, 4th edn. Academic Press, San Diego.

Phillis JW & Wu PH (1981). Catecholamines and the sodium pump in excitable cells. *Prog Neurobiol* **17**, 141–184.

Prince DA & Tseng GF (1993). Epileptogenesis in chronically injured cortex: in vitro studies. *J Neurophysiol* **69**, 1276–1291.

Rapport RL, Harris AB, Friel PN & Ojemann GA (1975). Human epileptic brain Na,K ATPase activity and phenytoin concentrations. *Arch Neurol* **32**, 549–554.

Reich CG, Mason SE & Alger BE (2004). Novel form of LTD induced by transient, partial inhibition of the Na,K-pump in rat hippocampal CA1 cells. *J Neurophysiol* **91**, 239–247.

Reime Kinjo E, Arida RM, Mara de Oliveira D & da Silva Fernandes MJ (2007). The Na^+/K^+ATPase activity is increased in the hippocampus after multiple status epilepticus induced by pilocarpine in developing rats. *Brain Res* **1138**, 203–207.

Richards KS, Bommert K, Szabo G & Miles R (2007). Differential expression of Na^+/K^+-ATPase α-subunits in mouse hippocampal interneurons and pyramidal cells. *J Physiol* **585**, 491–505.

Ross ST & Soltesz I (2000). Selective depolarization of interneurons in the early posttraumatic dentate gyrus: involvement of the Na^+/K^+-ATPase. *J Neurophysiol* **83**, 2916–2930.

Ross ST & Soltesz I (2001). Long-term plasticity in interneurons of the dentate gyrus. *Proc Natl Acad Sci USA* **98**, 8874–8879.

Salin P, Tseng GF, Hoffman S, Parada I & Prince DA (1995). Axonal sprouting in layer V pyramidal neurons of chronically injured cerebral cortex. *J Neurosci* **15**, 8234–8245.

Senatorov VV & Hu B (1997). Differential Na^+-K^+-ATPase activity in rat lemniscal and non-lemniscal auditory thalami. *J Physiol* **502**, 387–395.

Shyjan AW, Cena V, Klein DC & Levenson R (1990). Differential expression and enzymatic properties of the Na^+,K^+-ATPase $\alpha 3$ isoenzyme in rat pineal glands. *Proc Natl Acad Sci USA* **87**, 1178–1182.

Tamas G, Buhl EH & Somogyi P (1997). Massive autaptic self-innervation of GABAergic neurons in cat visual cortex. *J Neurosci* **17**, 6352–6364.

Q12

Tateno T & Robinson HPC (2004). Threshold firing frequency-current relationships of neurons in rat somatosensory cortex: Type 1 and Type 2 dynamics. *J Neurophysiol* **92**, 2283–2294.

Therien AG & Blostein R (2000). Mechanisms of sodium pump regulation. *Am J Physiol Cell Physiol* **279**, C541–C566.

Thompson SM & Prince DA (1986). Activation of electrogenic sodium pump in hippocampal CA1 neurons following glutamate-induced depolarization. *J Neurophysiol* **56**, 507–522.

Tseng GF & Prince DA (1993). Heterogeneity of rat corticospinal neurons. *J Comp Neurol* **335**, 92–108.

Vaillend C, Mason SE, Cuttle MF & Alger BE (2002). Mechanisms of neuronal hyperexcitability caused by partial inhibition of Na^+-K^+-ATPases in the rat CA1 hippocampal region. *J Neurophysiol* **88**, 2963–2978.

Xiang Z, Huguenard JR & Prince DA (1998). $GABA_A$ receptor-mediated currents in interneurons and pyramidal cells of rat visual cortex. *J Physiol* **506**, 715–730.

Author contributions

T.R.A.: collection, analysis and interpretation of data, drafting and revising the manuscript, final approval of the manuscript. J.R.H. and D.A.P.: drafting and revising the manuscript, conception and design of the experimental protocol, final approval of the manuscript.

Acknowledgements

We thank Isabel Parada for histological assistance. This work was supported by NIH grants NS12151 and NS59379.

Non-technical summary

The capacity of neurons to respond appropriately to normal and pathophysiological levels of excitation is dependent on their ability to establish, regulate and maintain their ionic and electrical homeostasis. The sodium–potassium ATPase (the 'sodium pump') is the enzyme primarily responsible for this task through its active transport of Na^+ and K^+ ions across the cell membrane. Sodium pump dysfunction has been implicated in numerous CNS disorders and often leads to enhanced neuronal excitation, as may occur in epilepsy. The sodium pump is activated by increases in intracellular Na^+ that result from synaptic depolarization and cell firing, making its actions particularly important in cells that discharge at high frequencies, such as fast-spiking inhibitory interneurons. The primary neuronal output of the cerebral cortex is through excitatory pyramidal neurons in layer V, whose activity is in turn tightly regulated by these inhibitory interneurons. We demonstrate that fast-spiking inhibitory interneurons possess uniquely high levels of Na^+–K^+ ATPase activity that may be vital in maintaining and regulating normal neuronal activity during periods of enhanced excitability.

Queries

Journal: TJP
Paper: tjp˙4180

Dear Author
During the copy-editing of your paper, the following queries arose. Please respond to these by marking up your proofs with the necessary changes/additions. Please write your answers on the query sheet if there is insufficient space on the page proofs. Please write clearly and follow the conventions shown on the corrections sheet. If returning the proof by fax do not write too close to the paper's edge. Please remember that illegible mark-ups may delay publication.

Query Reference	Query	Remarks
Q1	Na^+–K^+ used rather than Na^+/K^+ to be consistent with rest of text, OK?	
Q2	Reime Kinjo: Please check surname is now correct.	
Q3	Author: '$(\pi/2)$' correct for 'PI/2'	
Q4	'total sum of squares – residual sum of squares/total sum of squares.' OK or brackets required?	
Q5	D-APV – OK, as above rather than AP-V (and throughout)?	
Q6	'Average' replaced by 'mean (± S.E.M.)' throughout legends. Please confirm S.E.M. is OK. Would a use of statistics paragraph in the Methods be helpful?	
Q7	'with a mean (± S.E.M.) peak inward current of'– OK?	
Q8	Table 1: 'Mean age (*postnatal days*)' OK? Encompasses range so 'P' removed.	
Q9	Table 1 footnote: Values ± x are means ± S.E.M. – OK?	
Q10	FS interneurons showed more Na^+–K^+ ATPase charge than either PYR cell type ($P < 0.05$; Fig. 4C). – OK, rather than Fig. 5C?	
Q11	Fig. 4 legend: 'activity (DGR charge) (mean ± S.E.M.).' – OK?	
Q12	Reime Kinjo E: Surname changed, please check OK.	

WILEY-BLACKWELL

USING E-ANNOTATION TOOLS FOR ELECTRONIC PROOF CORRECTION

Required Software

Adobe Acrobat Professional or Acrobat Reader (version 7.0 or above) is required to e-annotate PDFs. Acrobat 8 Reader is a free download: http://www.adobe.com/products/acrobat/readstep2.html

Once you have Acrobat Reader 8 on your PC and open the proof, you will see the Commenting Toolbar (if it does not appear automatically go to Tools>Commenting>Commenting Toolbar). The Commenting Toolbar looks like this:

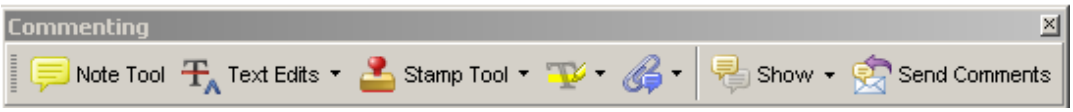

If you experience problems annotating files in Adobe Acrobat Reader 9 then you may need to change a preference setting in order to edit.

In the "Documents" category under "Edit – Preferences", please select the category 'Documents' and change the setting "PDF/A mode:" to "Never".

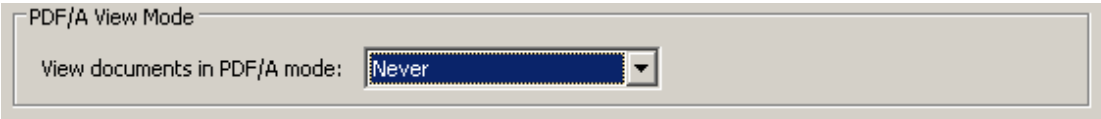

Note Tool — For making notes at specific points in the text

Marks a point on the paper where a note or question needs to be addressed.

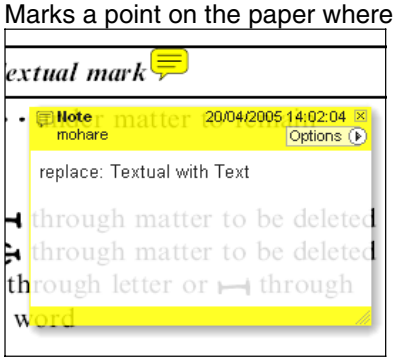

How to use it:

1. Right click into area of either inserted text or relevance to note
2. Select Add Note and a yellow speech bubble symbol and text box will appear
3. Type comment into the text box
4. Click the X in the top right hand corner of the note box to close.

Replacement text tool — For deleting one word/section of text and replacing it

Strikes red line through text and opens up a replacement text box.

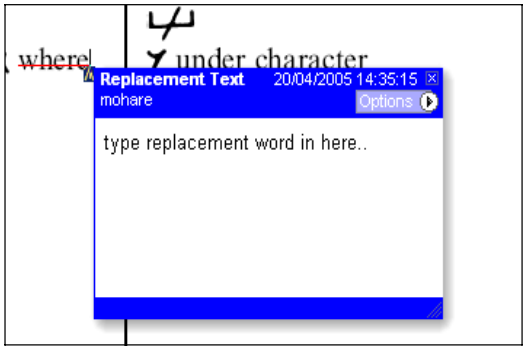

How to use it:

1. Select cursor from toolbar
2. Highlight word or sentence
3. Right click
4. Select Replace Text (Comment) option
5. Type replacement text in blue box
6. Click outside of the blue box to close

Cross out text tool — For deleting text when there is nothing to replace selection

Strikes through text in a red line.

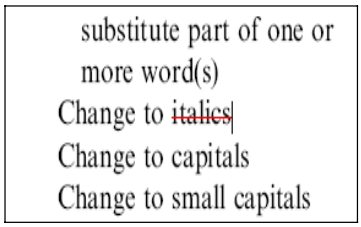

How to use it:

1. Select cursor from toolbar
2. Highlight word or sentence
3. Right click
4. Select Cross Out Text

WILEY-BLACKWELL

Approved tool — For approving a proof and that no corrections at all are required.

How to use it:

1. Click on the Stamp Tool in the toolbar
2. Select the Approved rubber stamp from the 'standard business' selection
3. Click on the text where you want to rubber stamp to appear (usually first page)

Highlight tool — For highlighting selection that should be changed to bold or italic.

Highlights text in yellow and opens up a text box.

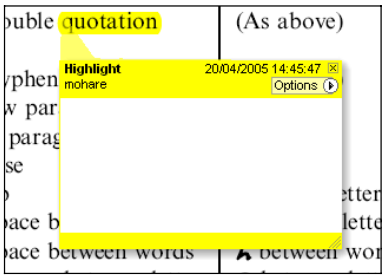

How to use it:

1. Select Highlighter Tool from the commenting toolbar
2. Highlight the desired text
3. Add a note detailing the required change

Attach File Tool — For inserting large amounts of text or replacement figures as a files.

Inserts symbol and speech bubble where a file has been inserted.

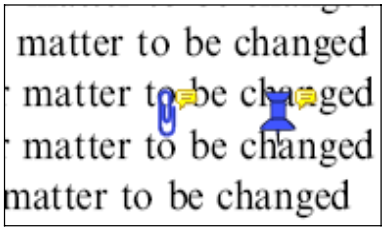

How to use it:

1. Click on paperclip icon in the commenting toolbar
2. Click where you want to insert the attachment
3. Select the saved file from your PC/network
4. Select appearance of icon (paperclip, graph, attachment or tag) and close

Pencil tool — For circling parts of figures or making freeform marks

Creates freeform shapes with a pencil tool. Particularly with graphics within the proof it may be useful to use the Drawing Markups toolbar. These tools allow you to draw circles, lines and comment on these marks.

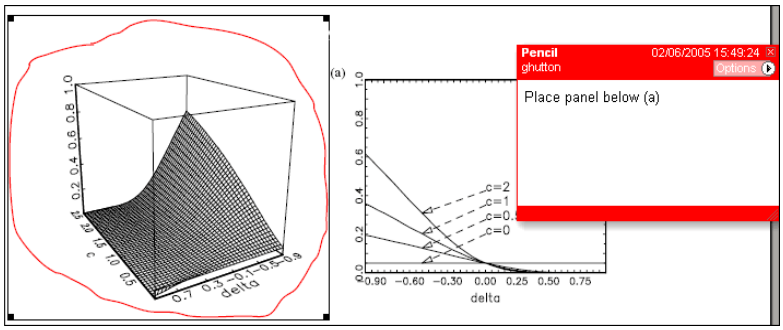

How to use it:

1. Select Tools > Drawing Markups > Pencil Tool
2. Draw with the cursor
3. Multiple pieces of pencil annotation can be grouped together
4. Once finished, move the cursor over the shape until an arrowhead appears and right click
5. Select Open Pop-Up Note and type in a details of required change
6. Click the X in the top right hand corner of the note box to close.

WILEY-BLACKWELL

Help

For further information on how to annotate proofs click on the Help button to activate a list of instructions:

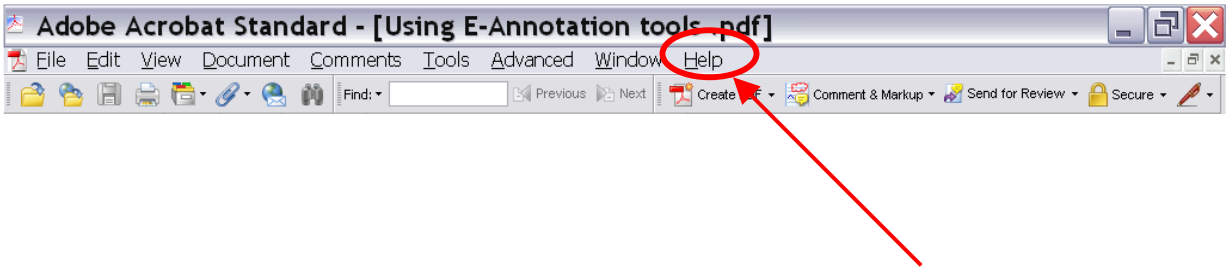

MARKED PROOF

Please correct and return this set

Please use the proof correction marks shown below for all alterations and corrections. If you wish to return your proof by fax you should ensure that all amendments are written clearly in dark ink and are made well within the page margins.

Instruction to printer	*Textual mark*	*Marginal mark*
Leave unchanged	··· under matter to remain	✓
Insert in text the matter indicated in the margin	⌇	New matter followed by ⌇ or ⌇ (x2)
Delete	/ through single character, rule or underline or ⊢⊣ through all characters to be deleted	⌇ or ⌇ (x2)
Substitute character or substitute part of one or more word(s)	/ through letter or ⊢⊣ through characters	new character / or new characters /
Change to italics	— under matter to be changed	⌒
Change to capitals	≡ under matter to be changed	≡
Change to small capitals	= under matter to be changed	=
Change to bold type	~ under matter to be changed	~
Change to bold italic	≈ under matter to be changed	≈
Change to lower case	Encircle matter to be changed	≠
Change italic to upright type	(As above)	⊬
Change bold to non-bold type	(As above)	⊬
Insert 'superior' character	/ through character or ⌇ where required	⌇ or ⌇ under character e.g. ⌇ or ⌇
Insert 'inferior' character	(As above)	⌇ over character e.g. ⌇
Insert full stop	(As above)	⊙
Insert comma	(As above)	,
Insert single quotation marks	(As above)	⌇ or ⌇ and/or ⌇ or ⌇
Insert double quotation marks	(As above)	⌇ or ⌇ and/or ⌇ or ⌇
Insert hyphen	(As above)	⊢
Start new paragraph	⌐	⌐
No new paragraph	⌒	⌒
Transpose	⌐¬	⌐¬
Close up	linking ⌒ characters	⌒
Insert or substitute space between characters or words	/ through character or ⌇ where required	Y
Reduce space between characters or words	| between characters or words affected	⊤